

# Design, Molecular Docking, Synthesis and Antiproliferative Evaluation of New 5-Aminoisatin Derivatives

Noor Waleed Ibrahim<sup>\*,1</sup>,  Monther Faisal Mahdi<sup>1</sup>  and  
Ayad M.R. Rauf<sup>2</sup> 

<sup>1</sup>Department of Pharmaceutical Chemistry, College of Pharmacy, Mustansiriyah University, Baghdad, Iraq.

<sup>2</sup>Department of Pharmaceutical Chemistry, College of Pharmacy, Farahidi University, Baghdad, Iraq.

\*Corresponding author

Received 26/7/2023, Accepted 7/4/2024, Published 20/9/2025



This work is licensed under a Creative Commons Attribution 4.0 International License.

## Abstract

Cancer is a disease triggered by an uncontrolled growth of a group of cells. Many cancers may be cured if diagnosed early and treated with surgery, radiation, chemotherapy, or immunotherapy. Chemotherapy is a common and systematic therapy that involves the use of anticancer drugs to treat cancer. Tyrosine kinase inhibitors have been shown to be effective in the treatment of cancers targeting tumorigenesis drivers. Two series of compounds derived from 5-aminoisatin Schiff bases IIa-c were synthesized IIIa-c that contain one CH<sub>3</sub> group & IVa-c which contain two CH<sub>3</sub> group. The role of tyrosine kinase in the control of cellular growth and differentiation inhibitors and their potential in clinical application are well documented by dramatic examples like, Gleevec, Iressa and Herceptin. The proposed compounds were successfully synthesized and purified; they were characterized and identified using: melting point, IR spectroscopy, <sup>1</sup>H-NMR and <sup>13</sup>C-NMR; The *in vitro* cytotoxic activity of these novel compounds was tested and molecular docking-based *in silico* tyrosine kinase selectivity via GOLD Suite (v.5.7.1); Our docking results and the experimental data (*In vitro* study) are in good accord since the compound IIIa shows the highest docking result and at the same time showing a promising cytotoxic activity among the tested compounds when tested against (A549) cancer cell lines by the MTT assay in comparison with erlotinib. Additionally, ADME studies were conducted to determine which of them are candidates for oral administration, their absorption location, bioavailability, topological polar surface area, and drug-likeness.

**Keywords:** 5-Aminoisatin, ADME, Docking, GOLD, Lipinski rule.

## Introduction

Isatins are synthetically versatile substrates that may be utilized to make a wide range of heterocyclic compounds such as indoles and quinolines, as well as as a raw material for medication development<sup>(1&2)</sup>. Isatin derivatives are known to have a variety of biological effects such as antimicrobial activities<sup>(3)</sup>, anticonvulsant activity<sup>(4)</sup>, antiproliferative activity<sup>(5&6)</sup>, anti-inflammatory activity<sup>(7)</sup>, antioxidant activity<sup>(8)</sup>, anthelmintic activity<sup>(9)</sup>. Cancer is the most horrible disease and, after cardiovascular illnesses, the second leading cause of mortality worldwide<sup>(10)</sup>; Because the disease is so complex, it can't be simply treated with only one or a few medications<sup>(11)</sup>. Because cancer can arise in so many various places in the human anatomy, medical applications, therapies, and drugs might be challenging to target an ever-changing disease<sup>(12)</sup>; Since the malignant growth cells can attack the neighbouring and distant tissues via the circulation. A tumor is three types benign, pre-malignant or malignant. A benign tumor does not spread into non-adjacent tissues. Pre-malign is the pre-cancerous condition. Malignancy is the condition, in which tumors become very bad and results in death of human being<sup>(13)</sup>. In advanced stages, a malignant growth patient may die because of either ill-advised finding or treatment disappointment<sup>(14)</sup>. Radiotherapy and surgery are commonly used in the early stages of cancer; chemotherapy is a cancer treatment options at an advanced stage of the disease<sup>(15)</sup>. Despite recent improvements in cancer treatment such as individualized therapy and innovative immunotherapeutics, overall survival rates have not increased appreciably. The development of resistance to cancer-fighting medications is a key barrier to the present therapy regimes' failure<sup>(16)</sup>. Primary (intrinsic) and secondary (acquired) resistance to cancer therapy are the two types of resistance. The lack of an objective clinical response following medication is a sign of primary resistance. Secondary resistance, on the other hand, refers to a local or distant return of the tumour following a clinical remission<sup>(17)</sup>. Computational methods provide another way to address drug resistance, especially the identification of mechanisms of resistance<sup>(18)</sup>. Molecular docking has become a crucial step in the drug discovery process, with

the goal of predicting the binding mechanism and affinity of the protein-ligand complex <sup>(19)</sup>. Tyrosine kinase inhibitors are classified as types I, II, allosteric, substrate directed, and covalent inhibitors based on their mode of action <sup>(20)</sup>

The development of new and varied cancer medications made it possible to treat cancer cells that had previously been resistant to an older treatment <sup>(21)</sup>, our goal is to design and synthesize the best fitted structures as a new tyrosine kinase inhibitors achieved with the soft wares and prediction of anticancer activity utilizing a modern software supplied by the Cambridge Crystallographic Data Centre and to examine those tyrosine kinase inhibitors on a specific (A549) cancer cell line cultures .

## Materials and Methods

### Chemicals and reagents

All reagents and anhydrous solvents were analytical grade, and they were used exactly as they were acquired from commercial suppliers (U.K., Spain, Germany, China, BDH and England). 5-Aminoisatin was supplied by the ChemShuttle Company, United States.

### Instrumentation

Melting points were determined by open capillary method on Stuart/ Electrothermal an electric melting point apparatus (U.K.) and. IR spectra were recorded on a FT-IR spectrophotometer Shimadzu as KBr disks at Mustansiriyah University -College of Pharmacy. <sup>1</sup>H NMR spectra were recorded using DMSO-d<sub>6</sub> as solvent and TMS as internal standard on a Bruker (400 MHz)& Varian 500 MHz spectrometer (Chemical shifts represented in  $\delta$ , ppm). <sup>13</sup>C NMR spectra were recorded on a Bruker (75.65 MHz) & Varian (125.65 MHz) spectrometer. Cytotoxicity assay was performed at the tissue culture center/ pharmacology and toxicology department/ College of Pharmacy, Mustansiriyah University using trypsin/EDTA, RPMI 1640, fetal bovine serum (Fisher scientific , USA); [ MTT 3-(4,5-dimethyl-2-thiazolyl)-2,5-diphenyl -2H-tetrazoliumbromide] (Fisher scientific , USA); dimethyl sulfoxide (DMSO-SantacruzBiotechnology, Dallas, TX, USA); phosphate-buffered saline (PBS)( Gibco, USA); CO<sub>2</sub> incubator and laminar flow hood (Memert, Germany ); Autoclave (Astell, Germany); Freezer -20 °C( Crafft, Korea); Freezer -80 °C( Gel, Germany).

### Chemical synthesis

#### General procedure for the synthesis of 5-aminoisatin schiff bases (IIa-c)

Aromatic amines (3 mmol) and 5-amino isatin hydrochloride (0.5958 gm, 3 mmol) were added to ethanol (10 mL) in a round bottomed flask, the mixture was heated during the first few minutes to about 50°C, then add 1 mL of glacial acetic acid

drop by drop. The mixture was continued to be heated with stirring at 79 °C under reflux for 4 hrs; mixture cooled to room temperature. The resulting solid was collected by filtration, washed with absolute ethanol and dried in open air. The result compounds were added to solution of 3ml of (1.5 mmol, 0.0074 gm) K<sub>2</sub>CO<sub>3</sub> dissolved in distilled water and after stirring for a few minutes was filtered; washed with water, dried and recrystallized from absolute ethanol <sup>(22)</sup>.

#### 4-((5-amino-2-oxindolin-3-ylidene)amino)benzoic acid(IIa)

Physical properties: Reddish brown (70.7% yield); m.p. 188-190°C;

FT-IR: 3418, 3337cm<sup>-1</sup> v (NH<sub>2</sub> of isatin), 3240 cm<sup>-1</sup> v (NH), 1734 cm<sup>-1</sup> v (C=O), 1657 cm<sup>-1</sup> v (C=N).

<sup>1</sup>H-NMR: 5.80ppm (s,2H, NH<sub>2</sub>), 6.55ppm (d,1H, Ar-H), 6.58ppm (s,1H, Ar-H), 6.93ppm (d,2H, Ar-H), 6.97ppm (d,1H, Ar-H), 7.65ppm (d,2H, Ar-H), 10.96 ppm (s,1H, NH) and 11.92ppm (s,1H,OH).

<sup>13</sup>C-NMR:(113.05, 113.25, 113.76, 116.45, 117.38, 123.76, 131.69, 144.63, 145.36, 153.61, 156.49, 163.67 and 167.97) ppm.

#### 5-amino-3-((4-hydroxyphenyl)imino)indolin-2-one (IIb)

Physical properties: Reddish brown (72.6% yield); m.p. 174-175°C;

FT-IR: 3520cm<sup>-1</sup> v(OH), 3485, 3339cm<sup>-1</sup> v(NH<sub>2</sub> of isatin), 3175cm<sup>-1</sup> v (NH), 1734 cm<sup>-1</sup> v (C=O), 1661 cm<sup>-1</sup> v (C=N).

<sup>1</sup>H-NMR: 5.80ppm (s,2H, NH<sub>2</sub>), 6.52 ppm (d,2H, Ar-H), 6.62ppm (d,1H, Ar-H), 6.92ppm (s,1H, Ar-H), 6.96ppm (d,2H, Ar-H), 6.99ppm (d,1H, Ar-H), 10.45 ppm (s,1H, OH) and 10.96ppm (s,1H,NH).

<sup>13</sup>C-NMR:(113.23, 113.39, 116.09, 116.47, 120.52, 123.76, 144.61, 145.37, 151.12, 156.49 and 163.67) ppm.

#### 5-amino-3-((4-bromophenyl)imino)indolin-2-one (IIc)

Physical properties: Reddish brown (63.7% yield); m.p. 190-192°C;

FT-IR:3429, 3275cm<sup>-1</sup> v(NH<sub>2</sub> of isatin), 3148 cm<sup>-1</sup> v(NH), 1732cm<sup>-1</sup> v(C=O), 1661 cm<sup>-1</sup> v(C=N)and845cm<sup>-1</sup> v(C-Br).

<sup>1</sup>H-NMR: 5.83ppm (s,2H, NH<sub>2</sub>), 6.55 ppm (d,1H, Ar-H), 6.90ppm (d,2H, Ar-H), 6.94ppm (s,1H, Ar-H), 6.97ppm (d,1H, Ar-H), 7.15ppm (d,2H, Ar-H) and 10.94ppm (s,1H,NH).

<sup>13</sup>C-NMR:(106.56, 113.17, 113.85, 116.27,116.52, 123.54, 131.78, 144.55, 145.44, 148.51, 156.48and 163.67) ppm.

#### General procedure for the synthesis of ureido derivatives of 5- aminoisatin Schiff bases( IIIa-c&IVa-c)

Compounds (IIa-c) (1 mmol) was added to 10mL dichloromethane / methanol in a ratio of (9:1). The mixture was cooled to 10 °C the appropriate substituted aromatic isocyanates (1mmol) was added slowly. The mixture was stirred at room

temperature for 4 hrs. and left in the refrigerator overnight. Solid products IIIa-c&IVa-c were separated out from the mixture, washed with dichloromethane, allowed to air dried and recrystallized from absolute ethanol<sup>(23)</sup>.

**4-((2-oxo-5-(3-(*m*-tolyl)ureido)indolin-3-ylidene)amino)benzoic acid(IIIa)**

Physical properties: Orange (85% yield); m.p. 301°C;

FT-IR: 3398, 3302 cm<sup>-1</sup> v (NH of urea&2-oxoindolin), 1736 cm<sup>-1</sup> v (C=O), 1634 cm<sup>-1</sup> v (C=N and C=O of urea) and 1554 cm<sup>-1</sup> v (NH deformation in urea).

<sup>1</sup>H-NMR: 2.30ppm (s,3H, CH<sub>3</sub>), 6.78 ppm (d,1H, Ar-H), 6.81ppm (t,1H, Ar-H), 6.99ppm (s,1H, Ar-H), 7.17ppm (d,1H, Ar-H), 7.19ppm (d,2H, Ar-H), 7.23ppm (d,2H, Ar-H), 7.25ppm (s,1H, Ar-H), 7.33ppm (d,2H, Ar-H), 7.66ppm (s,1H, NH ureido), 8.59 ppm (s,1H, NH ureido), 10.99ppm (s,1H,NH) and 11.64ppm (s,1H,OH).

<sup>13</sup>C-NMR:(21.71, 113.04, 113.35, 113.69, 115.81, 116.39, 119.15, 122.99, 123.97, 129.08, 131.68, 138.41, 140.15, 144.72, 145.29, 150.09, 152.98, 156.50, 163.68 and 167.97) ppm.

**1-(3-((4-hydroxyphenyl)imino)-2-oxoindolin-5-yl)-3-(*m*-tolyl)urea(IIIb)**

Physical properties: Reddish orange (82.3% yield); m.p. 290-292°C;

FT-IR: 3487cm<sup>-1</sup> v (OH), 3348, 3181 cm<sup>-1</sup> v (NH of urea&2-oxoindolin), 1732 cm<sup>-1</sup> v (C=O), 1659 cm<sup>-1</sup> v (C=N and C=O of urea).

<sup>1</sup>H-NMR: 2.29ppm (s,3H, CH<sub>3</sub>), 6.28 ppm (d,2H, Ar-H), 6.50ppm (d,1H, Ar-H), 6.62ppm (t,1H, Ar-H), 6.87ppm (m,3H, Ar-H), 6.93ppm (d,1H, Ar-H), 6.97 ppm (d,2H, Ar-H), 7.00ppm (s,1H, Ar-H), 7.97ppm (s,1H, NH ureido), 8.58 ppm (s,1H, NH ureido), 10.44ppm (s,1H,OH) and 10.97ppm (s,1H,NH).

<sup>13</sup>C-NMR:(21.71, 113.28, 113.74, 116.43, 119.37, 123.82, 138.41, 140.13, 144.66, 145.33, 150.10, 152.85, 156.49 and 163.67) ppm.

**1-(3-((4-bromophenyl)imino)-2-oxoindolin-5-yl)-3-(*m*-tolyl)urea(IIIc)**

Physical properties: Reddish brown (70.8% yield); m.p. 287-289°C;

FT-IR: 3283, 3184 cm<sup>-1</sup> v (NH of urea&2-oxoindolin), 1732 cm<sup>-1</sup> v (C=O), 1659 cm<sup>-1</sup> v (C=N and C=O of urea) and 844cm<sup>-1</sup> v(C-Br).

<sup>1</sup>H-NMR: 2.30ppm (s,3H, CH<sub>3</sub>), 6.79 ppm (d,1H, Ar-H), 6.82ppm (m,3H, Ar-H), 7.15ppm (s,1H, Ar-H), 7.17ppm (d,1H, Ar-H), 7.20ppm (d,2H, Ar-H), 7.23ppm (s,2H, Ar-H), 7.26ppm (s,1H, Ar-H),

7.33ppm (s,1H, NH ureido), 8.58 ppm (s,1H, NH ureido) and 10.98ppm (s,1H,NH).

<sup>13</sup>C-NMR:(21.71, 113.26, 113.78, 115.82, 119.16, 123.00, 129.08, 131.87, 138.42,140.14, 150.43, 152.98and 163.50) ppm.

**4-((5-(3-(2,6-dimethylphenyl)ureido)-2-oxoindolin-3-ylidene)amino)benzoic acid(IVa)**

Physical properties: Reddish orange (81.2% yield); m.p. 304 dec.°C;

FT-IR: 3279, 3219 cm<sup>-1</sup> v (NH of urea&2-oxoindolin), 1731 cm<sup>-1</sup> v (C=O), 1650 cm<sup>-1</sup> v (C=N and C=O of urea).

<sup>1</sup>H-NMR: 2.26ppm (s,6H, CH<sub>3</sub>), 6.55ppm (m,3H, Ar-H), 6.94ppm (d,2H, Ar-H), 6.98ppm (d,2H, Ar-H), 7.01ppm (s,1H, Ar-H), 7.06ppm (d,2H, Ar-H), 7.65ppm (s,1H, NH ureido), 8.66 ppm (s,1H, NH ureido), 10.97ppm (s,1H,NH) and 11.95ppm(s,1H, OH).

<sup>13</sup>C-NMR:(18.67, 113.04, 113.30, 113.71, 116.41, 117.37, 123.88, 128.12, 131.69, 144.68,145.31, 150.00, 153.62, 156.49, 163.67 and 167.97) ppm.

**1-(2,6-dimethylphenyl)-3-(3-((4-hydroxyphenyl)imino)-2-oxoindolin-5-yl)urea(IVb)**

Physical properties: Reddish orange (78.6% yield); m.p. 305-307°C;

FT-IR: 3477cm<sup>-1</sup> v (OH), 3304, 3111 cm<sup>-1</sup> v (NH of urea&2-oxoindolin), 1732 cm<sup>-1</sup> v (C=O), 1659 cm<sup>-1</sup> v (C=N and C=O of urea).

<sup>1</sup>H-NMR: 2.26ppm (s,6H, CH<sub>3</sub>), 6.45 ppm (d,2H, Ar-H), 6.48 ppm (m,3H, Ar-H), 6.94ppm (d,2H, Ar-H), 6.97ppm (d,2H, Ar-H), 7.00ppm (s,1H, Ar-H), 7.89ppm (s,1H, NH ureido), 8.35ppm (s,1H, NH ureido), 10.44 ppm (s,1H, OH) and 10.97ppm (s,1H,NH).

<sup>13</sup>C-NMR:(18.68, 113.27, 113.75, 116.44, 123.79, 127.82, 132.19, 136.08, 144.65,145.34, 150.42, 152.81, 156.49 and 163.67) ppm.

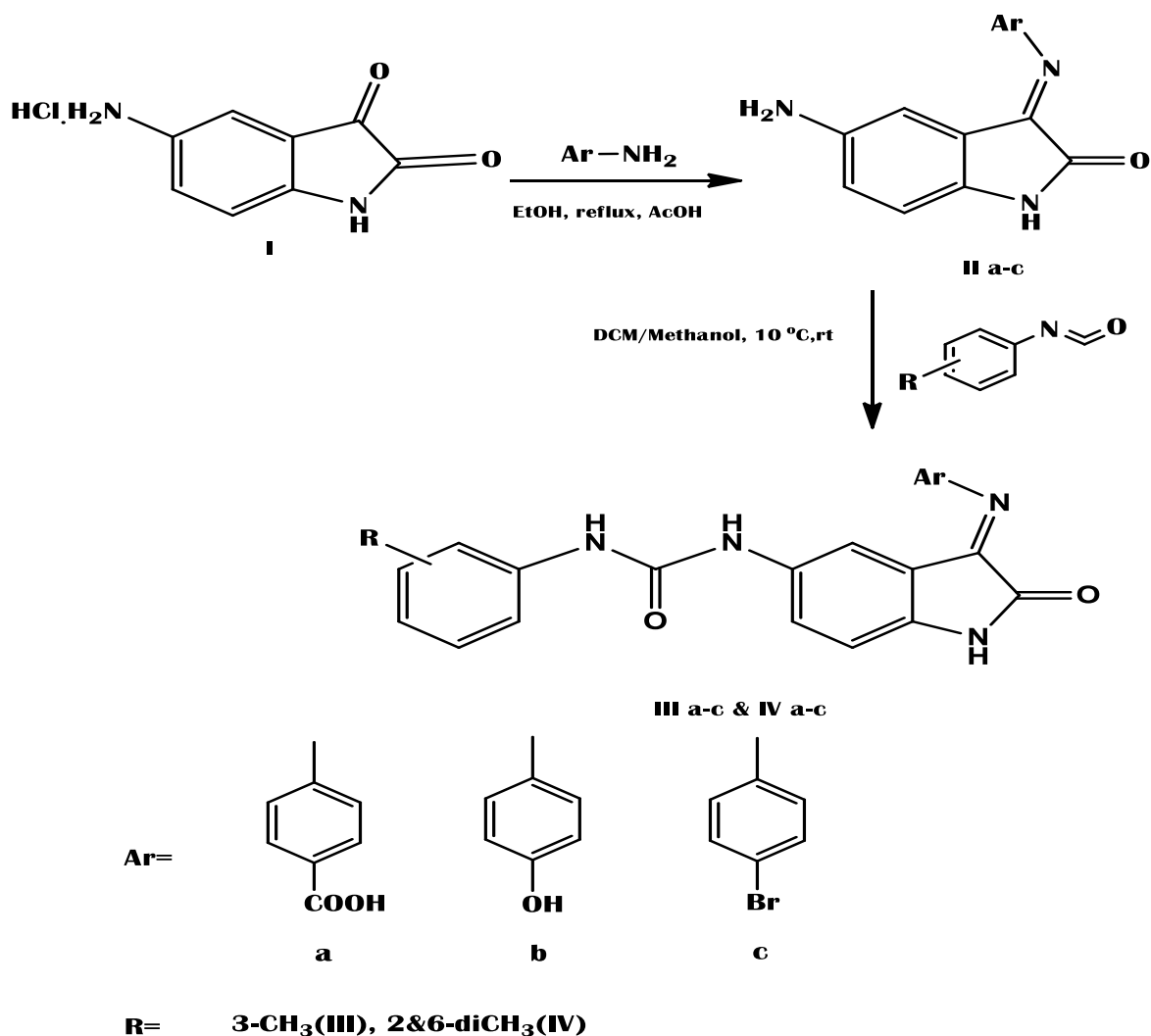
**1-(3-((4-bromophenyl)imino)-2-oxoindolin-5-yl)-3-(2,6-dimethylphenyl)urea(IVc)**

Physical properties: Reddish orange (73% yield); m.p. 313 dec.°C;

FT-IR: 3270 cm<sup>-1</sup> v (NH of urea&2-oxoindolin), 1731 cm<sup>-1</sup> v (C=O), 1649 cm<sup>-1</sup> v (C=N and C=O of urea) and 843 cm<sup>-1</sup> v(C-Br).

<sup>1</sup>H-NMR: 2.24ppm (s,6H, CH<sub>3</sub>), 6.50-6.52 ppm (d,2H, Ar-H), 6.97ppm (m,3H, Ar-H), 6.99ppm (d,2H, Ar-H), 7.05ppm (s,2H, Ar-H), 7.14ppm (s,1H, Ar-H), 7.96ppm (s,1H, NH ureido), 8.56 ppm (s,1H, NH ureido), 10.98ppm (s,1H,NH).

<sup>13</sup>C-NMR:(18.67, 113.31, 113.67, 116.25, 116.38, 123.92, 128.12, 131.79, 144.68,145.26, 150.04, 152.12, 156.48 and 163.67) ppm



Scheme 1. Synthesis of Schiff bases and target compounds

**Invitro cytotoxic activity**

The IC<sub>50</sub> value was defined as the lowest concentration of compound where percent inhibition is equal to 50. The determination of IC<sub>50</sub> values was done using nonlinear regression analysis (prism). Error bars represent the standard error of the mean% (SEM) for triplicate analysis.

The MTT colorimetric assay was used to estimate the effects of synthesized compounds (IIIa-c&IVa-c) on lung cancer cell viability. Cells suspension (100μL) were added into 96-well flat-bottom tissue culture plated at concentrations of (5 x 10<sup>3</sup> cells per well) and incubated for (24hr.) in standard conditions, (4 x 10<sup>3</sup> cells per well) for 48hr, and (3 x 10<sup>3</sup> cells per well) for 72hr incubation. Afterward, 24hr completed the cells were treated with 50 μM from each compound from each compound.

When a recovery period of 24hr, 48hr, and 72hr, completed the cell culture medium was removed and cultures were incubated for 4hr at 37 C° with a medium containing 20μL of MTT (of stock of 5mg/mL MTT/PBS from 30mL solution). After 4hr remove the supernatant and dispose it according

to the lab recommendations. Add 100μL of DMSO to each well to solubilize the crystals and tap the plates onto roll paper; leave the plates open and facing down to the paper at room temperature in the dark condition for about (15-20 min), and repeat this section in 48 and 72hr.

The assay was done in a triplicate and the optical density of each plate (well) was measured at a transmitting wavelength (520-600 nm) by using Multiscan Reader. The inhibition rate of cell growth (percentage of cytotoxicity) was calculated as follows:

$$[\text{Inhibition Rate percentage}] = \frac{(A - B)}{A} * 100$$

Where [A, and B] referred to the optical density of control & tested compounds respectively<sup>(24)</sup>.

Our final compounds were Investigated for their inhibitory action on cancerous cells using unique cell line cultures and hence no need for animal trial or even for human volunteers at the meanwhile, we use liver, prostate and lung cancer cells and we notice that the better results of inhibition is on the lung cancer cells. We use erlotinib as comparator because the protein that we

obtained from protein data bank was linked with erlotinib so when we remove this ligand from the protein and re dock with our compounds we can make a good comparison.

### Computational methods

#### A. Molecular docking

The molecular docking studies for the compounds were carried out using the CCDC GOLD Suite (v.5.7.1). The protein, ligands, hydrogen bonding interactions, short contacts, and bond length computation were all visualized using CCDC Hermes visualizer program (v. 1.10.1). ChemBioOffice (v. 17.1) was used to draw the chemical structures of our ligands<sup>(25&26)</sup>. Tyrosine kinase inhibitors have been shown to be effective in the treatment of cancers targeting tumorigenesis drivers.

#### B. ADME

With the help of the Swiss ADME server, the pharmacokinetic profile of the synthesized drugs, i.e. ADME, was predicted. All ligands (IIIa-c&IVa-c) were drawn by Chem Sketch (v. 12), converted to SMILE name by Swiss ADME tool which forecasts physicochemical characteristics as well as pharmacokinetic properties. The small molecule's lipophilicity and polarity were calculated using BOILEDDEG<sup>(27)</sup>.

## Results and Discussion

### Chemical synthesis

5- aminoisatin Schiff bases (IIa-c) were synthesized by cyclocondensation reaction using conventional method; compounds (IIIa-c&IVa-c) were synthesized by reacting 5-aminoisatin Schiff bases (IIa-c) with the appropriate aromatic isocyanates. The synthesized compounds were characterized by FT-IR, <sup>1</sup>H NMR and <sup>13</sup>C NMR techniques. The IR spectrum of Schiff bases (IIa-c) showed disappearance of absorption band due to  $\nu$  (C=O) ketone of 2-oxoindolin at 1763  $\text{cm}^{-1}$  and appearance of  $\nu$  (C=N) absorption band at (1660-

1657)  $\text{cm}^{-1}$  is an evidence of Schiff bases formation. The spectrum shows other bands at (3485-3275)  $\text{cm}^{-1}$ ; (3240-3148)  $\text{cm}^{-1}$ ; (1734-1732)  $\text{cm}^{-1}$ ; due to  $\nu$  (NH<sub>2</sub>) of isatin,  $\nu$  (NH) of oxoindole and  $\nu$  (C=O) of oxoindole respectively.

<sup>1</sup>H-NMR spectra of compounds (IIa-c) showed singlet signal at  $\delta$  = (10.96-10.94) ppm due to (NH) proton of 2-oxoindolin; and signals at  $\delta$  = (7.65-6.52) ppm due to aromatic protons and singlet signal at  $\delta$  = (5.83-5.80) ppm due to NH<sub>2</sub> of isatin. <sup>1</sup>H-NMR spectrum data of compound IIa& IIb showed singlet signal at  $\delta$  = (11.92&10.45) ppm respectively due to proton of hydroxyl group; <sup>13</sup>C-NMR spectral data of compounds (IIa-c) showed disappearance of signal at  $\delta$  = (185.89) ppm due to ketonic (C=O) of 2-oxoindolin and appearance of signal at  $\delta$  = (163.67) ppm due to (C=N). While the FTIR spectra of compounds (IIIa-c&IVa-c) showed disappearance of absorption band due to  $\nu$  (NH<sub>2</sub>) of isatin at (3485-3275)  $\text{cm}^{-1}$  and the appearance of absorption band due to  $\nu$  (NH) symmetric stretching and  $\nu$  (C=O) of urea at (3398-3181)  $\text{cm}^{-1}$ ; (1659-1634) respectively.

<sup>1</sup>H-NMR spectra of compounds (IIIa-c&IVa-c) showed two singlet signal at  $\delta$  = (8.66-8.35)& (7.97-7.33) ppm due to (NH) proton of ureido group; singlet signal at  $\delta$  = (2.24-2.30) ppm due to protons of CH<sub>3</sub> substitution on (ring D) also the spectrum showed disappearance of signal at  $\delta$  = (5.83-5.80) ppm due to NH<sub>2</sub> of isatin, <sup>13</sup>C-NMR spectra of compounds (IIIa-c&IVa-c) showed appearance of signal at  $\delta$  = (152.12-153.62) ppm due to (C=O) of ureido group and signal at  $\delta$  = (21.71-18.67) ppm due to carbon of CH<sub>3</sub> substitution.

### Invitro cytotoxic activity:

The obtained data revealed that from the newly synthesized compounds [IIIa& IVa] had an inhibitory activity against EGFR-TK with a relative inhibition percentage (35&40.9  $\mu\text{M}$ ) respectively that was close to the approved drug, erlotinib(25.23  $\mu\text{M}$ ).

**Table 1. Cell death percentage of compounds IIIa-c & IVa-c as compared with erlotinib**

Compounds	% of Cell death in 24hr	% of Cell death in 48hr	% of Cell death in 72hr
Erlotinib	68.60	77.10	82.40
IIIa	62.97	78.43	81.21
IIIb	25.09	28.50	30.66
IIIc	30.09	38.50	44.66
IVa	44.50	65.40	75.30
IVb	28.32	35.6	41.81
IVc	19.97	22.43	28.21

Table 2. Time response dose of compounds IIIa-c & IVa-c as compared with erlotinib

<p>compound (IIIa)</p>	<p>compound IIIa</p> <table border="1"> <thead> <tr> <th>Time (hours)</th> <th>IIIa (% Cell Death)</th> <th>Erlotinib (% Cell Death)</th> </tr> </thead> <tbody> <tr> <td>24</td> <td>62</td> <td>68</td> </tr> <tr> <td>48</td> <td>78</td> <td>78</td> </tr> <tr> <td>72</td> <td>82</td> <td>82</td> </tr> </tbody> </table>	Time (hours)	IIIa (% Cell Death)	Erlotinib (% Cell Death)	24	62	68	48	78	78	72	82	82
Time (hours)	IIIa (% Cell Death)	Erlotinib (% Cell Death)											
24	62	68											
48	78	78											
72	82	82											
<p>compound (IIIb)</p>	<p>compound IIIb</p> <table border="1"> <thead> <tr> <th>Time (hours)</th> <th>IIIb (% Cell Death)</th> <th>Erlotinib (% Cell Death)</th> </tr> </thead> <tbody> <tr> <td>24</td> <td>25</td> <td>68</td> </tr> <tr> <td>48</td> <td>28</td> <td>78</td> </tr> <tr> <td>72</td> <td>30</td> <td>82</td> </tr> </tbody> </table>	Time (hours)	IIIb (% Cell Death)	Erlotinib (% Cell Death)	24	25	68	48	28	78	72	30	82
Time (hours)	IIIb (% Cell Death)	Erlotinib (% Cell Death)											
24	25	68											
48	28	78											
72	30	82											
<p>Compound (IIIc)</p>	<p>compound IIIc</p> <table border="1"> <thead> <tr> <th>Time (hours)</th> <th>IIIc (% Cell Death)</th> <th>Erlotinib (% Cell Death)</th> </tr> </thead> <tbody> <tr> <td>24</td> <td>30</td> <td>68</td> </tr> <tr> <td>48</td> <td>38</td> <td>78</td> </tr> <tr> <td>72</td> <td>45</td> <td>82</td> </tr> </tbody> </table>	Time (hours)	IIIc (% Cell Death)	Erlotinib (% Cell Death)	24	30	68	48	38	78	72	45	82
Time (hours)	IIIc (% Cell Death)	Erlotinib (% Cell Death)											
24	30	68											
48	38	78											
72	45	82											
<p>compound (IVa)</p>	<p>compound IVa</p> <table border="1"> <thead> <tr> <th>Time (hours)</th> <th>IVa (% Cell Death)</th> <th>Erlotinib (% Cell Death)</th> </tr> </thead> <tbody> <tr> <td>24</td> <td>45</td> <td>68</td> </tr> <tr> <td>48</td> <td>65</td> <td>78</td> </tr> <tr> <td>72</td> <td>75</td> <td>82</td> </tr> </tbody> </table>	Time (hours)	IVa (% Cell Death)	Erlotinib (% Cell Death)	24	45	68	48	65	78	72	75	82
Time (hours)	IVa (% Cell Death)	Erlotinib (% Cell Death)											
24	45	68											
48	65	78											
72	75	82											

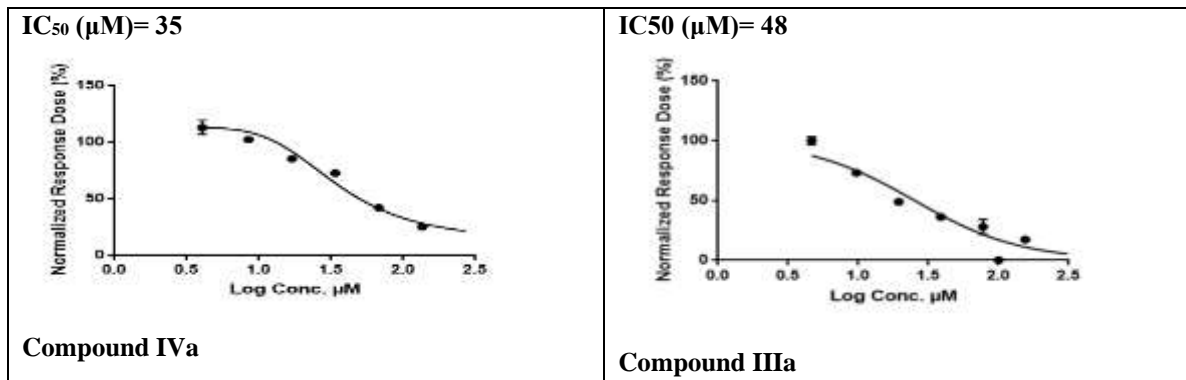
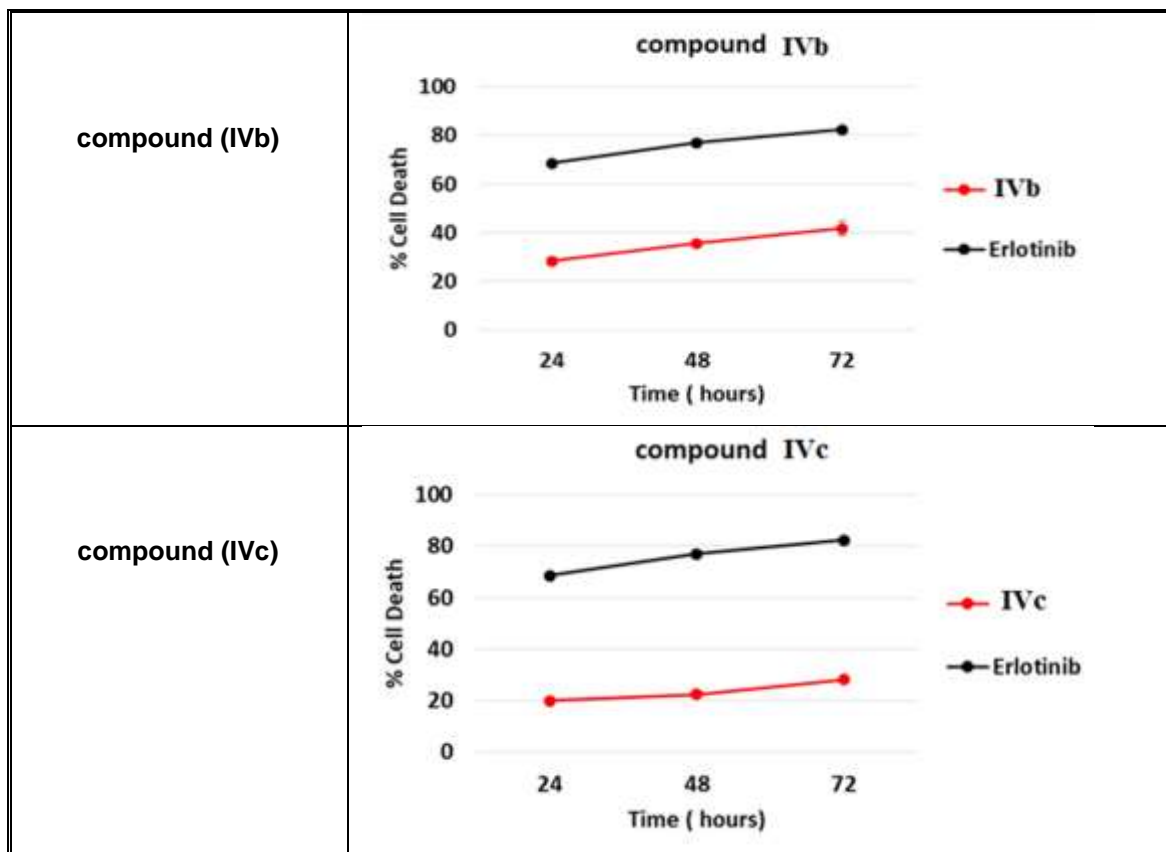


**Figure 1.** Dose-response curves of IC<sub>50</sub> for compounds [IIIa& IVa], treated for 72hr. with different ranges of concentrations (100, 50, 25, 12.5, 6.25, 3.125, 1.562, 0.781, 0.390, and, 0.195 μM)<sup>(28)</sup>. The normalized dose-response was plotted with log concentrations of compounds [IIIa& IVa]. The determination of IC<sub>50</sub> values was done using nonlinear regression analysis (prism). Error bars represent the standard error of the mean% (SEM) for triplicate analysis.

**Docking study**

Furthermore, our docked results and the experimental data (*In vitro* study) are in close accord

since the compound [IIIa] that show the highest docking results are the same that show a promising antitumor activity among the tested compounds.

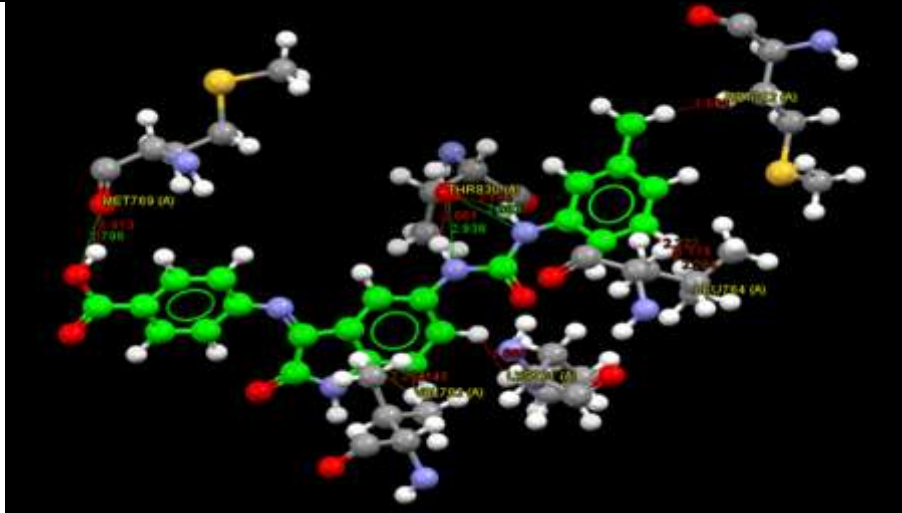
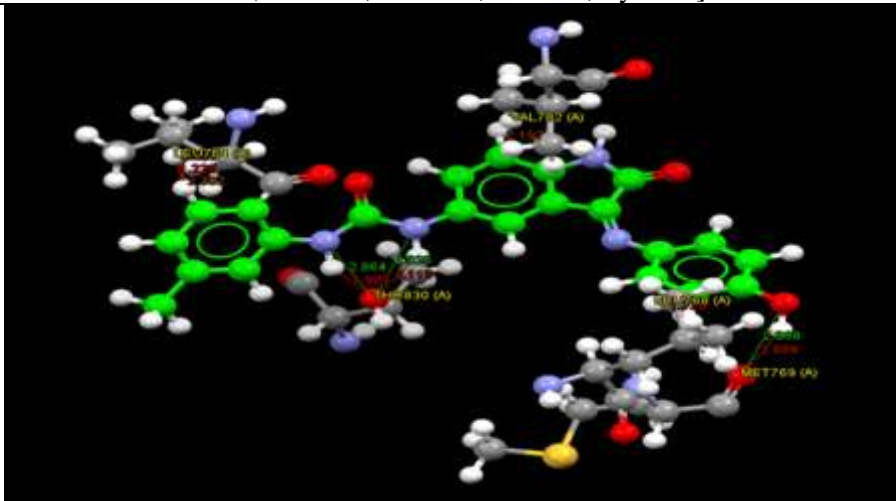
**Table 3. Docking result of 5-aminoisatin derivatives and standard TKIs Erlotinib docked with EGFR(PDB code: 4HJO).**

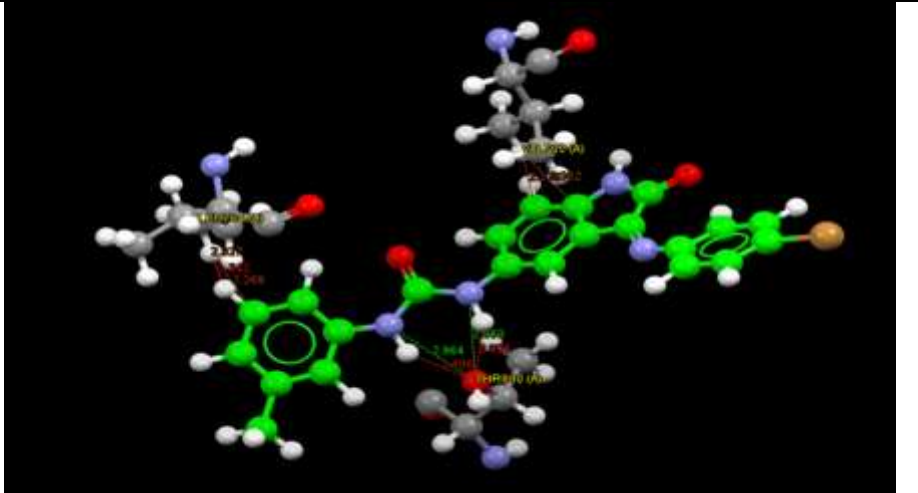
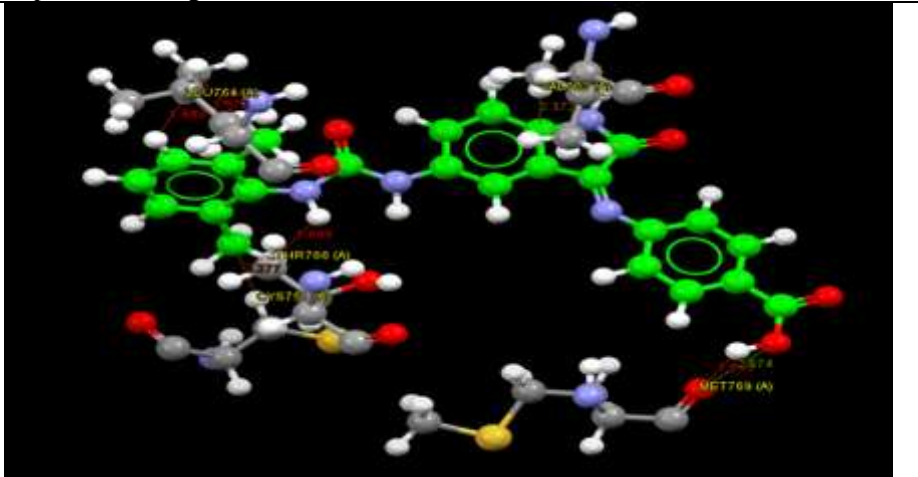
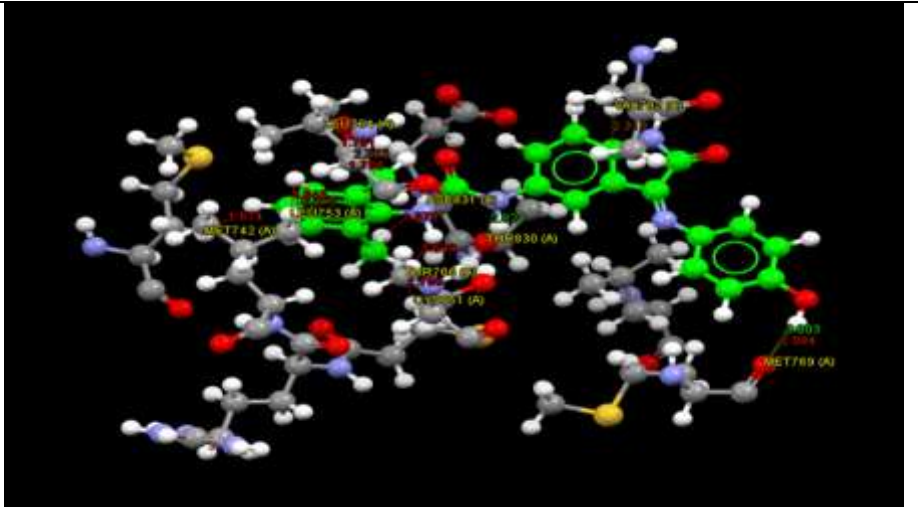
<b>Compounds</b>	<b>EGFR Binding Energy (PLP Fitness) (kcal/mol)</b>	<b>Amino Acids Included in H- bonding</b>	<b>Amino Acids Included in short contact Interactions</b>
<b>IIIa</b>	<b>89.26</b>	<b>Thr 830 (2)* Met 769</b>	<b>Met 742 Thr 830 (2)* Leu 764 (3)* Met 769 Val 702 (2)* Lys 721</b>
<b>IIIb</b>	<b>83.21</b>	<b>Thr 830(2)* Met 769</b>	<b>Met 769 Leu 768 Thr 830 (2)* Leu 764 (3)* Val 702</b>
<b>IIIc</b>	<b>83.96</b>	<b>Thr 830 (2)*</b>	<b>Thr830(2)* Leu764 (3)* Val702 (2)*</b>
<b>Iva</b>	<b>80.78</b>	<b>Met 769</b>	<b>Thr 766 Cys 751 Leu 764(3)* Met 769 Val 702</b>
<b>IVb</b>	<b>79.99</b>	<b>Thr 830 Met 769</b>	<b>Met 769 Val 702 Leu 753(2)* Met 742 Thr 766 Asp 831 Cys 751 Leu 764(3)*</b>
<b>IVc</b>	<b>73.32</b>	<b>Thr 830(2)* Thr 766</b>	<b>Leu 764 (3)* Val 702 Asp 831(2)* Thr 766 Arg 817</b>

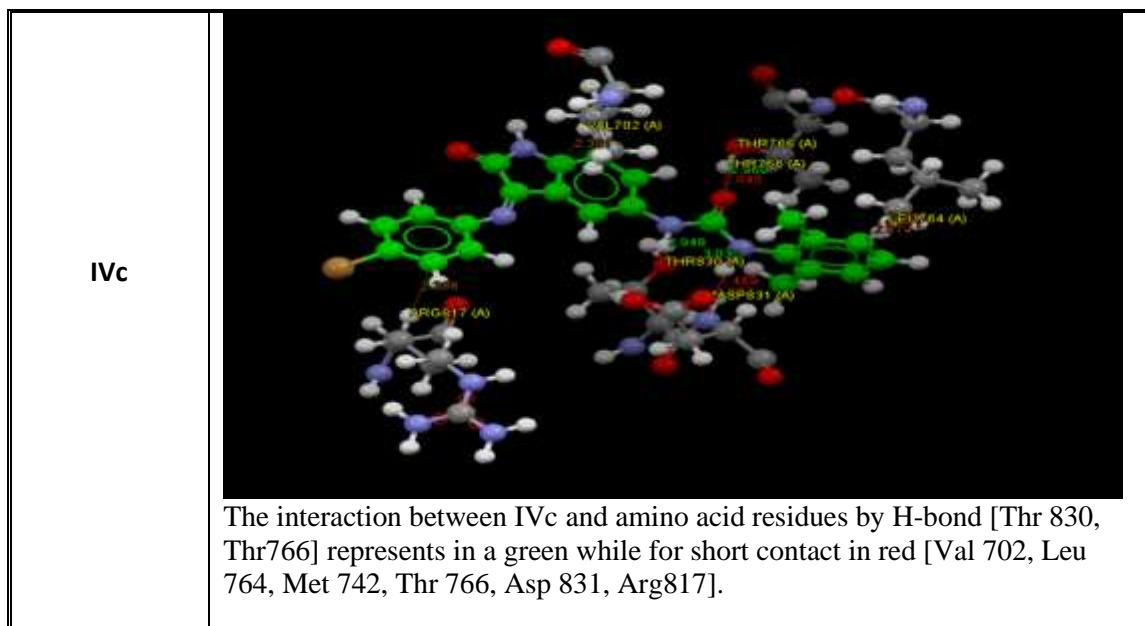
Erlotinib	83.94	Met 769	Gly695(2)*
		Lys 704	Lys 692
			Leu 694 (2)*
			Met 769
			Leu 764

\*Number in brackets refers to the number of bonds with the same amino acid.

**Table 4. H-bond and short contact interaction profile for the final compounds binding with EGFR receptor (PDB code: 4HJO). [ ball and stick style, amino acid residues in a gray ball and stick style]**

IIIa	 <p>The interaction between IIIa and amino acid residues by H-bond [Thr 830, Met 769] represents in a green while for short contact in red [Met 742, Thr 830, Leu 764, Met 769, Val 702, Lys 721] .</p>
IIIb	 <p>The interaction between IIIb and amino acid residues by H-bond [Thr 830, Met 769] represents in a green while for short contact in red [Met 769, Leu 768 ,Thr 830, Leu 764, Val 702]</p>

<p><b>IIIc</b></p>	 <p>The interaction between IIIc and amino acid residues by H-bond [Thr 830] represents in a green while for short contact in red [Thr830, Leu764, Val702]</p>
<p><b>IVa</b></p>	 <p>The interaction between IVa and amino acid residues by H-bond [Met 769] represents in a green while for short contact in red [Thr 766, Cys 751, Leu 764, Met 769, Val 702].</p>
<p><b>IVb</b></p>	 <p>The interaction between IVb and amino acid residues by H-bond [Thr 830, Met 769] represents in a green while for short contact in red [Met 769, Val 702, Leu 753, Met 742, Thr 766, Asp 831, Cys 751, Leu 764].</p>



**ADME Studies**

We assessed all synthesized compounds' pharmacokinetic properties (absorption, distribution, metabolism and excretion). Topological polar surface area (TPSA) was estimated, which is a very useful descriptor to estimate some ADME properties specially the degree of drug bioavailability and brain access (29). Thus, the molecules with a TPSA >140 Å² are thought to have low gastrointestinal absorption. The

results of all our synthesized compounds showed that TPSA values less than 140, which are in the range (82.59 –119.89) and the bioavailability for all ligands is in the range (0.55 –0.56) This means that all ligands make their way into the systemic circulation, as shown in the Table 5.

All the final compounds (IIIa-c&IVa-c) fulfilled Lipinski rule, it also fulfilled the topological descriptors and fingerprints of molecular drug-likeness structure keys as Log P and Log S.

**Table 5. The synthesized compounds' ADME characteristics profile**

Compounds	Formula	M.Wt (g/mol)	H-bond acceptors	H-bond donors	Log p	Log s	Molar Refractivity [MR]	TPSA	GI Abs.	BBB permeant	Lipinski violations
IIIa	C <sub>23</sub> H <sub>18</sub> N <sub>4</sub> O <sub>4</sub>	414.42	5	4	3.11	-7.68	121.11	119.89Å <sup>2</sup>	high	No	0
IIIb	C <sub>22</sub> H <sub>18</sub> N <sub>4</sub> O <sub>3</sub>	386.41	4	4	3.17	-7.75	116.18	102.82Å <sup>2</sup>	high	No	0
IIIc	C <sub>22</sub> H <sub>17</sub> BrN <sub>4</sub> O <sub>2</sub>	449.31	3	3	4.33	-9.12	121.85	82.59Å <sup>2</sup>	high	No	0
Iva	C <sub>24</sub> H <sub>20</sub> N <sub>4</sub> O <sub>4</sub>	428.45	5	4	3.64	-8.05	126.08	119.89Å <sup>2</sup>	high	No	0
IVb	C <sub>23</sub> H <sub>20</sub> N <sub>4</sub> O <sub>3</sub>	400.44	4	4	3.69	-8.13	121.14	102.82Å <sup>2</sup>	high	No	0
IVc	C <sub>23</sub> H <sub>19</sub> BrN <sub>4</sub> O <sub>2</sub>	463.34	3	3	4.85	-9.50	126.82	82.59Å <sup>2</sup>	high	No	0

**Conclusion**

Compounds (IIIa-c&IVa-c) effects on human A549 (lung) cancer cell line that is examined by MTT colorimetric assay showed that compounds IIIa&IVa have inhibitory activity against EGFR-TK with inhibition percentage for compound IIIa comparable to the standard drug erlotinib and these results correspond to the results in the Gold program. Also, ADME studies showed all final

compounds (IIIa-c&IVa-c) fulfilled the Lipinski rule, and all synthesized compounds absorbed from GIT. Those results prove the successful synthesis of the designed compounds.

## Recommendations for Further Future Work

1. Study cytotoxicity of the final compounds against other types of cell-line.
2. The antimicrobial activity for the final derivatives can be evaluated to identify their expected antibacterial & antifungal activity.
3. Promoted intramolecular cyclization of Schiff bases.

## Acknowledgment

The authors would like to thank Mustansiriyah University (www.uomustansiriyah.edu.iq) Baghdad- Iraq for its support in the present work.

## Conflicts of Interest

The authors declare that they have no conflicts of interest related to this work.

## Funding

The authors received no financial support for the research, authorship and/or publication of this article

## Ethics Statements

The study does not require ethical approval from an ethics committee.

## References

1. Rahul H. Profile of similarity of electron withdrawing structure towards analgesic-anti-inflammatory activity of the novel isatin analogue: design and implementation of phase I drug discovery. *International physiology journal*.2018; 1(2): 7.
2. Tariq A, Fazal R, Roh U, Asmat U, Fazal H, Farman UK, Mehwish K, Noor SK, Mudassir I. Synthesis and biological evaluation of isatin based thiazole derivatives. *BJSTR*. 2020 July; 28(5).
3. Vinod U, Harun P, Bijal P, Sanjay B. Benzofurano-isatins: Search for antimicrobial agents. *Arabian Journal of Chemistry*. 2017; 10: S389–S396.
4. Marzieh RK, Ahmad MF, Aref M, Alireza A. Synthesis and evaluation of anticonvulsant activity of (Z)-4-(2-oxoindolin-3-ylideneamino)-N-phenylbenzamide derivatives in mice. *Research in Pharmaceutical Sciences*. 2018 June; 13(3): 262-272.
5. Reem W, Aliyah A, Maha M, Adam K, Gary P, Mohamed A. New isatin–indole conjugates: synthesis, characterization, and a plausible mechanism of their in vitro antiproliferative activity. *Drug Design, Development and Therapy*. 2020;(14): 483–495.
6. Huda SS , Hatem AA, Iman SI, Amany ZM, Ali H, Md A, Motiur RAFM. Synthesis of novel potent biologically active N-benzylisatin-aryl hydrazones in comparison with lung cancer drug ‘gefitinib’. *Appl. Sci*. 2020 May; 10(3669).
7. Ravi J, Kiran G, Sarangapani M, Sriram R. Synthesis, in vivo anti-inflammatory activity, and molecular docking studies of new isatin derivatives. *International Journal of Medicinal Chemistry*. 2016.
8. Ozougwu, Jevan C. The Role of Reactive Oxygen Species and Antioxidants in Oxidative Stress. *International Journal of Research in Pharmacy and Biosciences*. 2016 June; 6(3): 1-8.
9. Aleti R, Srinivas MM. Synthesis, characterization, and anthelmintic activity of novel benzothiazole derivatives containing indole moieties. *Asian J Pharm Clin Res*. 2019; 3(12): 321-325.
10. Vaishali A, Katrin S, Mehak A, Ashif I, Ajay K, Saumya S, Anjana P, Satwinderjeet K, Hardeep ST. Drug targets in cellular processes of cancer: from nonclinical to preclinical models. Singapore: Springer; 2020.
11. Min L, Jianfeng J, Ruiqi W. Screening drug target combinations in disease-related molecular networks. *BMC Bioinformatics*. 2019; 20(7):129-151.
12. Saad HA. Synthesis, characterization, anticancer activity, and molecular docking of some new sugar hydrazine and arylidene derivatives. *Arabian Journal of Chemistry*. 2020; 13: 4771-4784.
13. G. Mahesh Kumar, K. Arun Kumar, P. Rajashekar Reddy, J. Tarun Kumar. A novel approach of tumor detection in brain using MRI scan images. *Research J. Pharm. and Tech*. 2020; 13(12):5914-5918.
14. Suhas SA, Santosh KS, Kiran AW. In vitro antioxidant potential and anticancer activity of ceratophyllum demersum Linn. extracts on HT-29 human colon cancer cell line. *Research J. Pharm. and Tech*. 2021; 14(1):28-36.
15. Aguslina K, Siswandono S, I Ketut S. Synthesis and Cytotoxic Activity of N-(4-bromo)-benzoyl-N’phenylthiourea and 4-(tert-butyl)-N-benzoylurea on Primary Cells of HER2-Positive Breast Cancer. *Research J. Pharm. and Tech*. 2021; 14(3):1195-1200.
16. Zuan-Fu L, Patrick CM. Emerging insights of tumor heterogeneity and drug resistance mechanisms in lung cancer targeted therapy. *Journal of Hematology & Oncology*. 2019; 12(134).
17. Jean- Christophe M, Sarah- Jane D, Mark AD. Non- genetic mechanisms of therapeutic resistance in cancer. *Nat Rev Cancer*. 2020 October 8.
18. Jinxin L, Jianfeng P, Luhua L. A combined computational and experimental strategy identifies mutations conferring resistance to

- drugs targeting the BCR-ABL fusion protein. *Communications Biology*. 2020; 3: 18.
19. S. Ramachandran, N. Vimeshya, K. Yogeshwaran, Binoy Varghese Cheriyan, M. Vijey Aanandhi. 6Molecular docking studies, synthesis, characterisation, and evaluation of azetidine-2-one derivative. *Research J. Pharm. and Tech*. 2021; 14(3):1571-1575.
  20. Samuel MD, Adeboye AO, Jamiu AA, Ajiboye OD, Tolulope OO Olaposi OI. Exploring receptor tyrosine kinases inhibitors in cancer treatments. *Egyptian Journal of Medical Human Genetics*; 2019: 20(35).
  21. Y. E. Matiichuk, T. I. Chaban, V. V. Ogurtsov, I. G. Chaban, V. S. Matiychuk. Antitumor Properties of Novel 2-(1H-Benzimidazol-2-yl)and 2-Benzothiazol-2-yl)-3-(5-phenylfuran-2-yl)-acrylonitriles Derivatives. *Research J. Pharm. and Tech*. 2020; 13(8):3690-3696.
  22. Kamaledin HE Tehrani, Maryam H, M H, Farzad K , Shohreh M. Synthesis and antibacterial activity of Schiff bases of 5-substituted isatins. *Chinese Chemical Letters*. 2016; 27: 221–225 .
  23. Rahul RK , Grace SC, Hsiao-CW, Chao-WY, Chiung-HH, On Lee , Chih-HC, Chrong-SH, Ching-HK, Nien-TC, Mai-WL, Ling-MW, Yen-CC , Tzong-HH, Chia-NC, Hui-CH, Hui CL, Ying-CS, Shuen-HC, Hsiang-WT, Chih-PL, Chia-MT, Tsan-LH, Yuan-JT, Ji-WC. Synthesis and structure–activity relationship of 6-aryureido-3-pyrrol-2-ylmethylideneindolin-2-one derivatives as potent receptor tyrosine kinase inhibitors. *Bioorganic & Medicinal Chemistry*. 2010; 18: 4674–4686.
  24. Shakila BS, Krishnamoorthy G, Senthamarai R, Mohamed JMS. Synthesis, spectral characterization and anticancer activity of novel pyrimidine derivatives. *Research J. Pharm. and Tech*. 2020; 13(12):6243-6247.
  25. Mustafa MA, Monther FM, Ayad MRR. Synthesis, anti-inflammatory, molecular docking and ADME studies of new derivatives of ketoprofen as cyclooxygenases inhibitor. *Al Mustansiriyah Journal of Pharmaceutical Sciences*. 2019; 19(4).
  26. Sarah SI, Monther FM, Basma MA. Molecular drug design, synthesis and antibacterial study of novel 4-oxothiazolidin-3-yl derivatives. *Al-Mustansiriyah Journal of Pharmaceutical Sciences*. 2020 June ; 20(2):1- 10.
  27. Daina A, Zoete V. A BOILED-Egg to predict gastrointestinal absorption and brain penetration of small molecules. *ChemMedChem*. 2016 Jun 6; 11(11):1117-21.
  28. Samuel AE, James S, Sarel FM, Alan C. Prioritization of anti-malarial hits from nature: chemo-informatic profiling of natural products with in vitro antiplasmodial activities and currently registered anti-malarial drugs. *Malar J*, 2016;15:50.
  29. Sebaugh JL. Guidelines for accurate EC50/IC50 estimation. *Pharm Stat*. 2011;10(2):128–34.

## تصميم وارساء جزيئي و تخليق و تقييم للفعالية المضادة للتكاثر لمشتقات جديدة لل-5-امينوايساتين

نور وليد ابراهيم<sup>1</sup>، منذر فيصل مهدي<sup>1</sup> و آياد محمد رشيد رؤوف<sup>2</sup>

<sup>1</sup> الجامعة المستنصرية، كلية الصيدلة، فرع الكيمياء الصيدلانية، العراق، بغداد.

<sup>2</sup> كلية الفراهيدي الجامعة، قسم الصيدلة، فرع الكيمياء الصيدلانية، العراق، بغداد.

### الخلاصة

السرطان هو مرض يبدأ بالنمو غير المنظم وغير المسيطر عليه لمجموعة من الخلايا . الكثير من انواع هذا المرض من الممكن ان تشفى ان شخصت مبكرا وعولجت بالعملية الجراحية، الاشعاع، العلاج الكيميائي والعلاج المناعي. العلاج الكيميائي هو علاج شائع و منهجي و الذي يشمل استعمال الادوية المضادة للسرطان لعلاجه، مثبطات التايروسين كيناز اظهرت انها فعالة في معالجة السرطانات باستهداف محركات التسرطن. سلسلتان من المركبات المشتقة من قاعدة الشيف لل 5-امينوايساتين IIa-c تم تخليقها IIIa-c التي تحتوي مجموعة CH<sub>3</sub> واحدة و IVa-c التي تحتوي مجموعتين من CH<sub>3</sub>. دور التايروسين كيناز في السيطرة على نمو و تمايز الخلايا اساسي لكل الكائنات الحية و قد وجد انه مشترك في الامراض السرطانية لدى الانسان. مثبطات التايروسين كيناز و فعاليتها في التطبيقات العلاجية ثبتت جيدا ب امثلة معروفة مثل جليفك، ايريزا و هيرسيتين. المركبات المقترحة تم تخليقها و تنقيتها بنجاح وتم توصيفها باستخدام نقاط النصف و قيم اطياف الترددات الراديوية، الشععة تحت الحمراء و الرنين المغناطيسي للبروتون و الكربون. تم تقييم هذه المركبات الجديدة من خلال نشاطها السام داخل الخلايا و كذلك انتقائيتها للتايروسين كيناز حاسوبيا عبر برنامج (GOLD) Suite (v.5.7.1) حيث كانت هذه النتائج متوافقة مع العمل المختبري على خط خلايا ؛ حيث ان المركب IIIa الذي امتلك اعلى نتائج حاسوبيا ببرنامج الدوكنك و بنفس الوقت اظهر نتائج واعدة مختبريا على الخلايا السرطانية من بين بقية المركبات المفحوصة عند استخدام اختبار قياس لوني لتقييم نشاط الخلايا الاستقلابي على خط خلايا A549 مقارنة بالمركب الاساسي الارلوتناب؛ كما تم اجراء دراسات (ADME) للتنبؤ اي من المركبات المصنعة يمكن اعطاؤها عن طريق الفم، موقع الامتصاص، التوافر البيولوجي، مساحة سطح القطب البيولوجية و الشبه الدوائي. الكلمات المفتاحية: 5-امينوايساتين، دراسة امتصاص و توزيع و اخرج المركبات ببرنامج ADME، النمذجة، برنامج جولد، قاعدة لينسكي.